Multi-scale integrative computational model the human atria and torso: a platform for the investigation of atrial fibrillation

Michael A Colman[1], Jonathan Stott[1], Oleg V Aslanidi[2], Phillip Langely[3], Henggui Zhang[1]

[1]*The University of Manchester,* [2]*King's College London, London,* [3]*University of Newcastle*

Correspondence: henggui.zhang@manchester.ac.uk, 0044161 306 3966, Oxford Road, M13 9PL, UK

I. INTRODUCTION

Atrial arrhythmias, including atrial fibrillation (AF), are characterised by irregular and rapid electrical activation of the atria. AF are the most common cardiac diseases and can lead to heart failure, stroke and even death (1). The mechanisms underlying the initiation and sustenance of AF, however, are incompletely understood. The human atria are electrically heterogeneous and structurally anisotropic. Dramatic regional differences in atrial action potential (AP) morphology and duration have been observed in both human and animal models (2). The fibrous structure of the atria also shows far less organization than in the ventricles. In this study we have developed a 3D model of the human atria and body surface ECG to investigate the underlying mechanisms of AF.

II. METHODS

The multi scale model of the human atria involved mapping previously developed heterogeneous single cell models for the AP (3) onto their respective regions of the atria (Fig 1. A, B). A recently reconstructed model for the human SAN geometry, fibre orientation and AP (4) was incorporated into the 3D atrial model (Fig 1. A, B). This model was then placed inside a torso geometry mesh (5) and the forward problem was solved by the use of a boundary element method (BEM) in order to simulate realistic ECG P-waves (Fig 1. C). Excitation propagation was simulated by using a mono-domain reaction-diffusion partial differential equation with use of higher order numerical solvers and an anisotropy ratio for conduction longitudinal and transverse to fibres of 10:1, respectively.

Re-entrant excitation wave (mimicking AF) was initiated by an s1-s2 pacing protocol: two s1 stimuli were applied at a cycle length of 350ms, followed by an s2 stimulus applied after 250ms. The stimulation site was selected at a region of both high electrical heterogeneity and anisotropy, at the junction between the crista terminalis (CT) and the pectinate muscles (PMs) in the right atrium. The model is then left to run for 10s.

The atrial model was validated by comparing atrial activation patterns to experimental data in both normal (6) and abnormal (3,7) conditions. The BSP model was validated by directly comparing the simulated data with experimental BSP maps (8) and ECG P-waves under normal conditions.

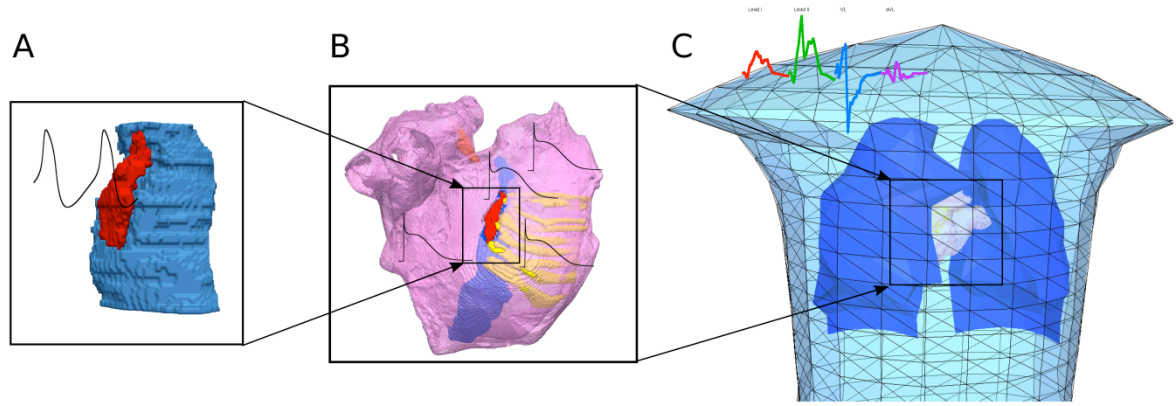

Figure 1. (A) Human sinoatrial node (SAN) geometry with representative AP displayed. (B) 3D heterogeneous anatomical model for the human atria with representative APs displayed over their respective regions. The SAN from A is incorporated into this model. (C) The 3D torso mesh model used to simulate the BSP, shown with the lungs and the orientation of the atria (shown in B). Representative ECG P-waves are displayed

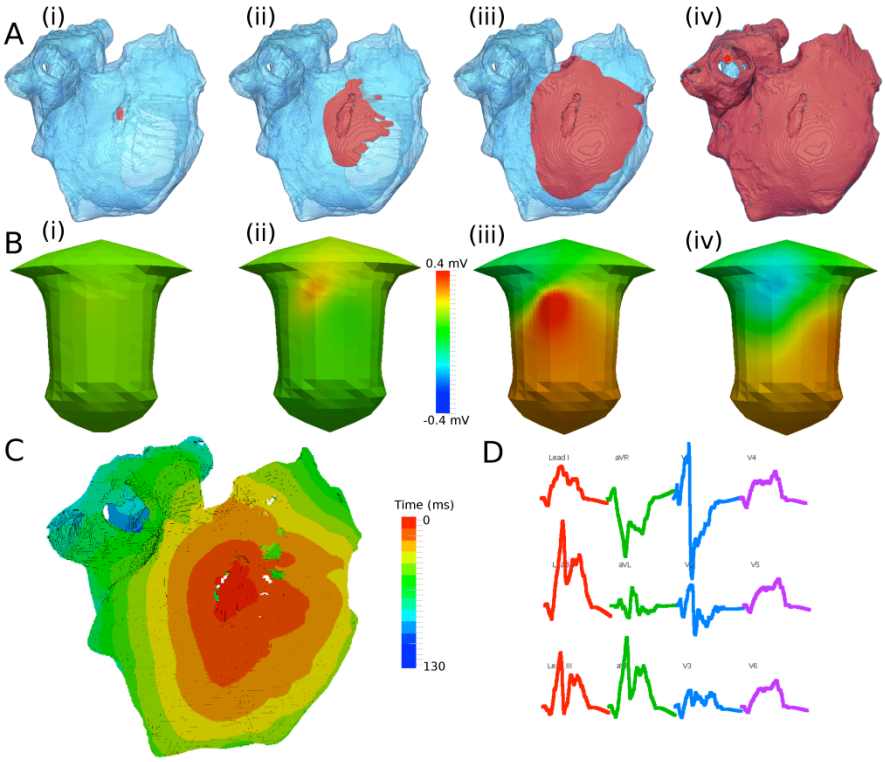

Figure 2. (A) Atrial excitation propagation. (B) BSP snapshots under normal conditions taken at i) 5 ms; ii) 25 ms; iii) 40 ms; and iv) 110 ms after the SAN initiates excitation. (C) Atrial activation pattern under normal conditions. (D) Corresponding P-wave profiles.

III. RESULTS

Fig. 2 shows the simulated electrical excitation conduction under the normal condition. Excitation is initiated in the centre of the SAN (Fig 2Ai). At the corresponding time, the BSP is largely uniform due to the lack of a propagating wave-front (Fig 2Bi). At 20ms, excitation has exited the SAN and propagates preferentially along the fibres orientated along the CT and PMs (Fig 2Aii). The corresponding BSP map shows a clear positive peak forming over the lower right lung due to this atrial propagation (Fig2Bii). At 40ms, a larger portion of the right atrium has been excited (Fig 2Aiii) and the dipole direction in the BSP can be clearly seen to point downwards and to the left (Fig2Biii). By 110ms, the right atrium has completely depolarized and the left atrium has almost been fully depolarized (Fig 2 A iv). As such, the peak of the BSP has disappeared and it begins to return to a largely uniform state (Fig 1Biv). The atrial activation map and corresponding P-waves are shown in Fig 2 panels C and D, respectively.

Fig 3A shows the initiation and break down of re-entrant waves following the s2 stimulus (see Methods). In Fig 3Ai, the application of the shortly coupled s2 stimulus at a region of high electrical heterogeneity results in a conduction block towards the CT; the longer AP duration in the CT relative to the PMs implies that the CT cells have not fully recovered at this time, and therefore cannot be stimulated. The PMs, however, have fully repolarised and therefore the wave-front can propagate within them. The excitation then circulates back into the CT after it has propagated for some time (Fig 3Aii) and the CT has had time to recover. This forms a ‘figure 8’ style re-entrant pattern. After ~100ms, however, the wave begins to break up due to the slow and fast conduction pathways resulting from the high level of anisotropy (Fig 3Aiii). By ~150ms the multiple re-entrant wavelets which characterize AF have begun to form. Fig 3B shows the long term behaviour of the model after the initiation of AF. The different snapshots in time, taken from the sixth and seventh second of simulation, demonstrate chaotic, multiple re-entrant wavelets which would result in a significant reduction in cardiac output. Representative BSP snapshots during this time are shown in Fig 3C and can be seen to be highly irregular. This re-entry was sustained throughout the entire 10s simulation.

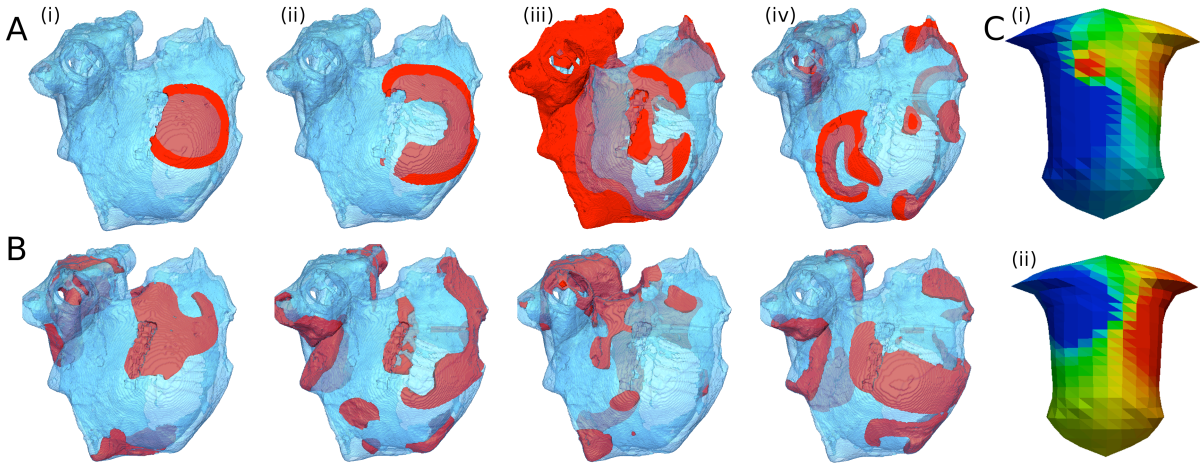

Figure 3. (A) Initiation and breakdown of a re-entrant wave following the s2 stimulus. Snapshots taken at i) 10ms; ii) 20 ms; iii) 100 ms; and iv) 150 ms after the stimulus. (B) Demonstration of multiple re-entrant wavelets characterizing AF. Snapshots taken at i) 605 ms; ii) 645 ms; iii) 690 ms; and iv) 735 ms after the s2 stimulus. (C) Snapshots of the BSP during AF.

IV. SUMMARY

A multi-scale biophysically detailed model of the human atria and torso has been developed. The model is validated under normal and abnormal conditions and is used to investigate the underlying mechanisms of AF. It is shown that heterogeneity and anisotropy both play a role in the initiation and sustenance of AF.

V. REFERENCES

1. Dobrev D, Nattel S. New insights into the molecular basis of atrial fibrillation: mechanistic and therapeutic implications. Cardiovasc. Res. 2011 Mar 1;89(4):689–91.

2. Nattel S, Shiroshita-Takeshita A, Brundel BJJM, Rivard L. Mechanisms of atrial fibrillation: lessons from animal models. Prog Cardiovasc Dis. 2005 Aug;48(1):9–28.

3. Colman MA, Aslanidi OV, Stott J, Holden AV, Zhang H. Correlation between P-wave morphology and origin of atrial focal tachycardia--insights from realistic models of the human atria and torso. IEEE Trans Biomed Eng. 2011 Oct;58(10):2952–5.

4. Chandler N, Aslanidi O, Buckley D, Inada S, Birchall S, Atkinson A, et al. Computer three-dimensional anatomical reconstruction of the human sinus node and a novel paranodal area. Anat Rec (Hoboken). 2011 Jun;294(6):970–9.

5. Weixue L, Ling X. Computer simulation of epicardial potentials using a heart-torso model with realistic geometry. IEEE Trans Biomed Eng. 1996 Feb;43(2):211–7.

6. Lemery R, Birnie D, Tang ASL, Green M, Gollob M, Hendry M, et al. Normal atrial activation and voltage during sinus rhythm in the human heart: an endocardial and epicardial mapping study in patients with a history of atrial fibrillation. J. Cardiovasc. Electrophysiol. 2007 Apr;18(4):402–8.

7. Kistler PM, Roberts-Thomson KC, Haqqani HM, Fynn SP, Singarayar S, Vohra JK, et al. P-wave morphology in focal atrial tachycardia: development of an algorithm to predict the anatomic site of origin. J. Am. Coll. Cardiol. 2006 Sep 5;48(5):1010–7.

8. Mirvis DM. Body surface distribution of electrical potential during atrial depolarization and repolarization. Circulation. 1980 Jul;62(1):167–73.